

# COSMOGLOBE DR1. II. First full-sky model of polarized synchrotron emission from all WMAP and Planck LFI data

U. Fuskeland<sup>1</sup>\* and D. Watts<sup>1</sup> et al.

Institute of Theoretical Astrophysics, University of Oslo, Blindern, Oslo, Norway

June 22, 2023

## ABSTRACT

We present the first statistically consistent model of full-sky polarized synchrotron emission derived from the combination of all *WMAP* and *Planck* LFI frequency maps. The basis of this analysis are the end-to-end reprocessed COSMOGLOBE Data Release 1 sky maps presented in a companion paper, which have significantly lower instrumental systematics than the legacy products from each experiment. We find that the resulting polarized synchrotron amplitude map has an average noise rms of  $2.4\mu\text{K}$  at 22 GHz and a smoothing scale of  $2^\circ$  FWHM, which is 30 % lower than the recently released BEYONDPLANCK model that included only LFI+*WMAP*  $Ka-V$  data, and it is 45 % lower than the raw *WMAP*  $K$ -band. The mean  $EE/BB$  power spectrum ratio is  $0.27 \pm 0.02$ , which agrees well with previous estimates from both *Planck* and QUIJOTE. Assuming a power law model for the synchrotron spectral energy density, we find a full-sky inverse noise-variance weighted mean of  $\beta_s = -3.06 \pm 0.08$  between *WMAP*  $K$ -band and LFI 30 GHz, in good agreement with previous estimates. At high Galactic latitudes, however, we find  $\beta_s = -3.31 \pm 0.08$ , which is slightly steeper than most previous foregrounds-oriented estimates, but in good agreement with the *Planck* 2018 LFI CMB likelihood result of  $\beta_s = -3.27 \pm 0.04$ . For comparison, the corresponding full-sky and high-latitude estimates derived from the official *WMAP* and LFI products are  $\beta_s = -3.44 \pm 0.08$  and  $\beta_s = -3.71 \pm 0.08$ , respectively. These values are obviously compromised by large-scale instrumental systematics in both *WMAP* and LFI. In summary, the novel COSMOGLOBE DR1 synchrotron model is both more sensitive and systematically cleaner than similar previous models, and it has a more complete error description that is defined by a set of Monte Carlo posterior samples. We believe that these products are preferable for all synchrotron-related scientific applications, including simulation, forecasting and component separation.

**Key words.** ISM: general – Cosmology: observations, polarization, cosmic microwave background, diffuse radiation – Galaxy: general

## Contents

|          |   |
|----------|---|
| <b>1</b> | <b>Introduction</b>                                   |
| <b>2</b> | <b>Data products</b>                                  |
| 2.1      | WMAP and Planck legacy data products . . . . .        |
| 2.2      | The Cosmoglobe data products . . . . .                |
| <b>3</b> | <b>Methods</b>  |
| 3.1      | T-T plot method . . . . .                             |
| 3.2      | T-T plot method with an ensemble of samples . . . . . |
| <b>4</b> | <b>Results for 23/30 GHz</b>                          |
| <b>5</b> | <b>Results for 23/33 GHz</b>                          |
| <b>6</b> | <b>Discussion and conclusion</b>                      |

### 1. Introduction

bla bla bla,

### 2. Data products

In this paper, we investigate the spatial variation of the polarized synchrotron spectral index, and specifically, we want to com-

pare the results using the legacy maps against the results using the COSMOGLOBE maps. The data products used are the *WMAP* and *Planck* maps in the 23–33 GHz regime. These frequencies are low enough so we can treat them as synchrotron tracers and hence ignore thermal dust and CMB, but not so low as we need to take into account effects like Faraday rotation (Fuskeland et al. 2021). The legacy data products and the data products from the COSMOGLOBE *WMAP* reanalysis (cite Watts et al. 2023), are described in the two following sections.

#### 2.1. WMAP and Planck legacy data products

The *WMAP* data products are available on the lambda archive<sup>1</sup>. As in Fuskeland et al. (2014), we use the *WMAP*  $K$  and  $Ka$  band Stokes  $Q$  and  $U$  parameter maps at 23 GHz and 33 GHz. The respective effective frequencies used are 22.45 GHz and 32.64 GHz. The maps originally at a HealPIX pixelization of  $N_{\text{side}} = 512$  are downgraded to  $N_{\text{side}} = 64$  and smoothed to a common resolution of  $1^\circ$  FWHM.

The *Planck* data products used are the  $Ka$  band Stokes  $Q$  and  $U$  maps at 30 GHz. We use an effective frequency of 28.4 GHz. Both the products from the *Planck* 2018 release (cite), and from the DR4? (cite-npipe) release are used, available on lambda. The products are natively at  $N_{\text{side}} = 1024$  ??, but as for the *WMAP* products, the maps are downgraded to  $N_{\text{side}} = 64$  and smoothed to  $1^\circ$  FWHM.

\* Corresponding author: U. Fuskeland; [unnif@astro.uio.no](mailto:unnif@astro.uio.no)

<sup>1</sup> <http://lambda.gsfc.nasa.gov>



**Fig. 1.** The sky is split into the same 24 regions as in Fuskeland et al. (2014). The most prominent point sources are masked out and shown as the grey circular areas.

(Show maps?)

## 2.2. The Cosmoglobe data products

COSMOGLOBE is a project? to do end-to-end analyses on several data sets jointly. Doing this can help to break the degeneracies of the different data sets, and in general improve on systematical effects. Being a end-to-end analysis means it goes all the way from Time ordered data (TOD) to cosmological parameters using the Bayesian Gibbs sampler, Commander3. For more details, see Watts et al 2023 and BeyondPlanck 2023. (Perhaps a bit short...)

What is relevant for this paper is some of the COSMOGLOBE end products produced by the reanalysis of the *WMAP* and *Planck* LFI time ordered data (TOD) (cite Watts 2023). This analysis produced new (improved?) *WMAP* and *Planck* LFI maps, which we will use in an analysis to compare to the legacy data. In particular, we are interested in exactly the same set of maps as in the previous section in order to be able to do a comparision study. So we use the maps in the 23-33 GHz regime, namely the *WMAP* 23 and 33 GHz and the *Planck* 30 GHz data. The pixelization and angular scale is the same as for the legacy products ( $N_{\text{side}} = 64$ ,  $1^\circ$  FWHM). The COSMOGLOBE end products consists of a series of many samples from the Gibbs chain, instead of just one mean sample as has been the normal case for previous data releases.

(Show maps? or do the other papers show a comparision of legacy vs cosmoglobe maps??)

## 3. Methods

### 3.1. T-T plot method

Short about the main T-T plot method here, but mainly refer to previous papers.

### 3.2. T-T plot method with an ensable of samples

Much better propagation of uncertainties with a whole suite of maps.

## 4. Results for 23/30 GHz

The uncertainty is calcuted as the minimum of the uncertainties in each rotation angle, and region. As in the Fuskeland 2021 paper, an systematic uncertainty that takes into account the variation of beta over rotation angle;  $[\max(\beta_{alpha}) - \min(\beta_{alpha})]/2$  is added in quadrature to the statistical uncertainty. For the Cosmoglobe analyses the standard deviation of the spectral indices for all samples is also added in quadrature to represent an additional systematic uncertainty.



**Fig. 2.** The spatial variation of the synchrotron spectral index, computed using T-T plot between the *WMAP* 23 GHz and *Planck* 2018 30 GHz (top), *WMAP* 23 GHz and *Planck* DR4 30 GHz (middle) and Cosmoglobe 23 GHz and Cosmoglobe 30 GHz (bottom). The spectral index is inverse variance weighted over rotation angle, and in the Cosmoglobe case also samples. Fix style of maps. Bottom figure will be updated using more samples.

$\min(\beta_{alpha})]/2$  is added in quadrature to the statistical uncertainty. For the Cosmoglobe analyses the standard deviation of the spectral indices for all samples is also added in quadrature to represent an additional systematic uncertainty.

## 5. Results for 23/33 GHz

We will also use Table 6, Figure (33) of Planck 2018 results IV Diffuse component separation

## 6. Discussion and conclusion

### References

- Fuskeland, U., Andersen, K. J., Aulien, R., et al. 2021, A&A, 646, A69  
Fuskeland, U., Wehus, I. K., Eriksen, H. K., & Næss, S. K. 2014, ApJ, 790, 104



**Fig. 3.** The synchrotron spectral index as a function of region number, computed using T-T plot between the 9-yr *WMAP* 23 GHz and *Planck* 2018 30 GHz (red), 9-yr *WMAP* 23 GHz and *Planck* DR4 30 GHz (blue) and Cosmoglobe 23 GHz and Cosmoglobe 30 GHz (black). The spectral index is inverse variance weighted over rotation angles, and samples. The horizontal line in the high latitude regions corresponds to the estimated spectral index values from the *Planck* 2018 likelihood analysis. [cite??](#) Figure will be updated using more samples.



**Fig. 4.** The synchrotron spectral index computed using T-T plot with the Cosmoglobe 23 GHz and 30 GHz data versus Cosmoglobe 23 GHz and 33 GHz data for the 24 regions. [Figure will be updated using more samples.](#)



**Fig. 5.** T-T plots for Stokes Q and U maps of the Cosmoglobe 23 GHz versus the Cosmoglobe 30 GHz (black) and the 9 yr WMAP 23 GHz versus Planck 2018 30 GHz (red) for all regions. The horizontal (solid and dotted) lines indicates the corresponding inverse variance weighted values of the spectral index, averaged over rotation angle. **Figure will be updated using more samples.**



**Fig. 6.** The synchrotron spectral index as a function of rotation angle, computed using T-T plot between the Cosmoglobe 23 GHz and the Cosmoglobe 30 GHz (black) compared to the spectral index using the 9 yr *WMAP* 23 GHz and *Planck* 2018 30 GHz (red) for all regions. The horizontal (solid and dotted) lines indicates the corresponding inverse variance weighted values of the spectral index. **Figure will be updated using more samples.**



**Fig. 7.** The spatial variation of the synchrotron spectral index, computed using T-T plot between the Cosmoglobe WMAP K band and Ka band. The spectral index is inverse variance weighted over rotation angle, and samples. Fix style of maps. Figure will be updated using more samples.



**Fig. 8.** The uncertainty of the synchrotron spectral index, computed using T-T plot between the Cosmoglobe WMAP K band and Ka band. REMOVE? Figure will be updated using more samples.



**Fig. 9.** The synchrotron spectral index, computed using T-T plot between the Cosmoglobe WMAP K band and Ka band (red) compared to the spectral index using the original 9 yr WMAP data (black) as a function of region number. The spectral index is inverse variance weighted over rotation angles, and samples. Figure will be updated, adding larger final uncertainty and using more samples.

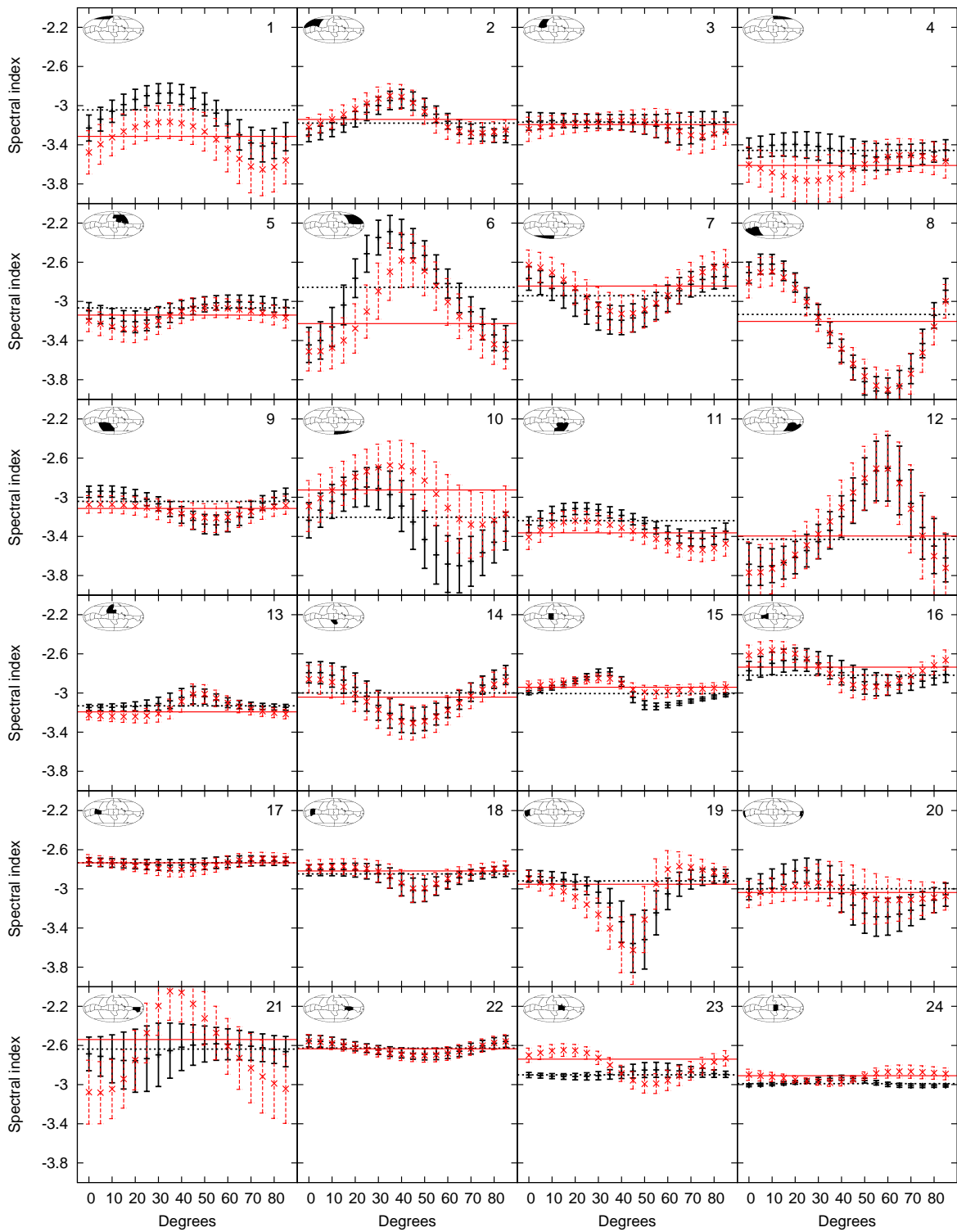


**Fig. 10.** The synchrotron spectral index as a function of rotation angle, computed using T-T plot between the Cosmoglobe WMAP K band and Ka band (red) compared to the spectral index using the original 9 yr WMAP data (black) for all regions. The horizontal lines indicates the corresponding inverse variance weighted values of the spectral index. **Figure will be updated using more samples.**